JOURNAL OF MATERIALS SCIENCE 20 (1985) 4006–4014

Influence of sulphidation on the metallic phase of an $Fe_{94}Si_6$ alloy

Z. ŻUREK
Institute of Inorganic Chemistry and Technology, Technical University, PL–31–155 Krakow, Poland

M. PRZYBYLSKI, S. M. DUBIEL*‡
*Institute of Metallurgy, Academy of Mining and Metallurgy, PL–30–059 Krakow, Poland and *Institut für Festkörperforschung der Kernforschungsanlage Jülich, Postfach 1913, D–5170 Jülich 1, West Germany*

Using X-ray phase analysis and microanalysis, optical and scanning electron microscopy, and Mössbauer-effect spectroscopy, the influence of sulphidation on the metallic phase of an $Fe_{94}Si_6$ alloy is studied. It has been revealed that three distinct layers are formed: (a) the outermost one, called the outer scale, is composed of FeS; (b) the next one, called the inner scale, also contains iron sulphide; and (c) the one occurring on the metallic core is enriched in silicon and contains an admixture of DO_3 structure. A possible mechanism responsible for the enrichment and for the formation of the DO_3 structure is proposed.

1. Introduction

It is expected that phenomena which occur in Fe–Si alloys during their sulphidation are different from those occurring due to oxidation of these alloys, because the affinities of iron and silicon to sulphur are very similar, while that of silicon to oxygen is much larger than that of iron to oxygen. Consequently, one expects that the process of selection and preferential oxidation of silicon that takes place during oxidation [1] does not occur during sulphidation. One can even expect an opposite effect to occur during sulphidation, namely that iron will sulphidize preferentially leading to enrichment of the surface zone of the core in silicon, assuming the concentration of the latter is low enough.

The high affinity of iron to silicon seems to be responsible for a formation of ordered structures (superstructures) in Fe–Si alloys. In particular the so-called DO_3 structure can be formed under certain heat treatment if the concentration of silicon amounts to 25%.

Its characteristic feature is that there are two nonequivalent iron sites, Fe_I and Fe_{II}. The former has four iron and four silicon atoms in the nearest-neighbour shell (NN) and six iron atoms in the next-nearest one (NNN), while the latter has only iron atoms in NN and only silicon atoms in NNN (a more detailed description of this superstructure will be given in Section 4). For other compositions of the alloy other superstructures can be formed, completely or partially, depending on the actual composition and heat treatment. Inden and Pitsch [2], for instance, based on the Bragg–Williams model explain the occurrence of these superstructures and determine their stability in terms of the temperature and composition.

A similar phenomenon of ordering was recently observed by Werber and Żurek for Cu–Si alloys [3]. The authors observed that the surface zone of the core of the sulphidized samples contained the η'-phase (Cu_3Si) which subsequently decayed into a metallic silicon.

In view of the above study it seems interesting to investigate the influence of sulphidation on

‡*Present address*: Laboratoire de Métallurgie, Ecole des Mines, Parc de Saurupt, F–54042 Nancy Cédex, France.

0022–2461/85 $03.00 + .12

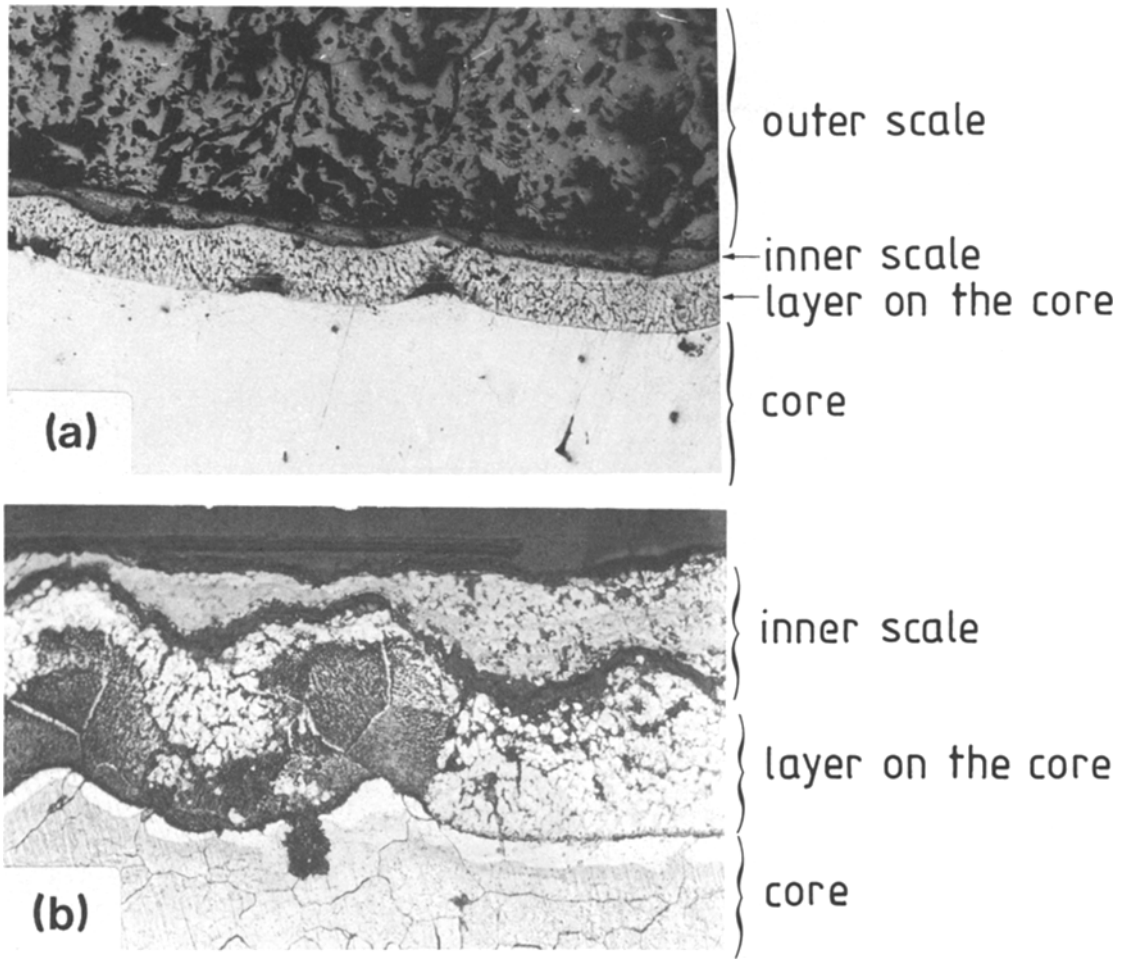

Figure 1 The microstructure obtained from the microsection of the sample sulphided at T_s = 800° C. (a) × 100, (b) × 250.

the metallic phase of the surface zone of Fe–Si alloys. In the following we present the results of such an investigation for an $Fe_{94}Si_6$ alloy, using X-ray phase analysis and microanalysis, optical and scanning electron microscopy, and Mössbauer-effect spectroscopy. Preliminary results have been presented elsewhere [4].

2. Experimental details

2.1. Alloy preparation, its sulphuration and sample preparation

An alloy whose final concentration of silicon was 6.1 at % was prepared by melting appropriate amounts of 99.99% purity iron and silicon in an induction furnace in an atmosphere of pure argon.

The resulting ingot was cold-rolled to 1.5 mm thickness. From the sheet rectangles of 20 mm × 30 mm size were cut out. Before sulphidation such samples were hand-ground with glasspapers of decreasing grains down to 5/0; they were then cleaned first with ethanol and next with acetone. Sulphidation was carried out in a sulphur vapour under a pressure of 1 atm using a set-up described previously [5]. The sulphidation lasted for 40 min at temperatures T_s = 600, 700 and 800° C, and was followed by cooling in air.

The morphology of a scale, the outer layer of the core and the inner part of the surface zone of the core was studied on microsections obtained by cutting samples perpendicular to the scale surface. In order to make grains more visible, microsections were etched in an alcoholic solution of nitric acid. Figs. 1 and 2 show the microstructure of the above-mentioned regions of interest for the samples sulphidized at 600 and 800° C respectively.

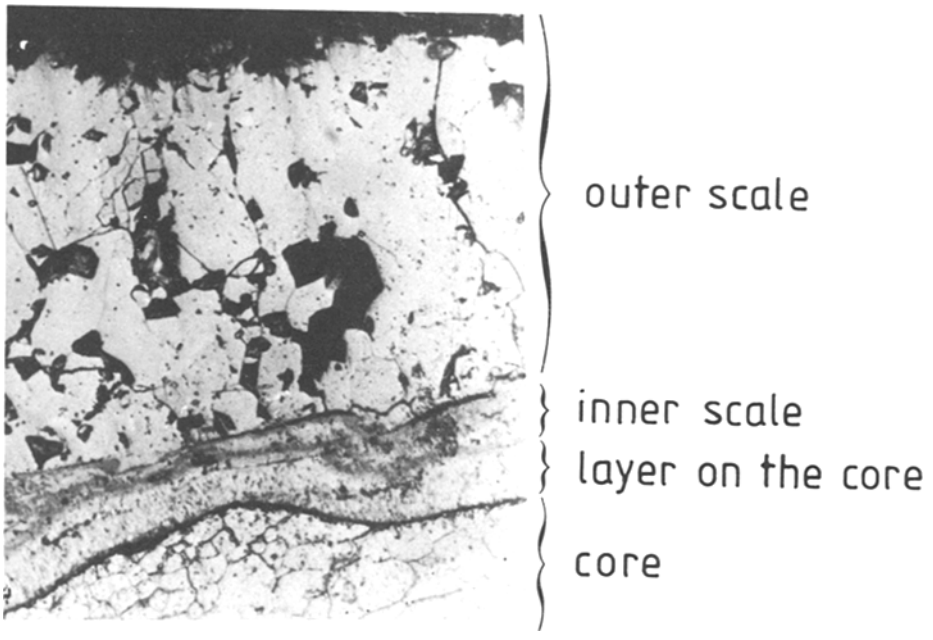

Figure 2 The microstructure obtained from the microsection of the sample sulphided at $T_s = 600°C$ (× 100).

For the analysis by means of a scanning electron microscope the samples were fractured perpendicularly to the sulphidized surface, and the geometry of the analysis was chosen in such a way that the electron beam was perpendicular to the area of the fracture. Figs. 3 to 5 present the microstructures of different layers of interest as obtained for the sample sulphidized at 800° C.

Distributions of elements in the layers of interest were obtained by means of the X-ray microanalyzer SMQ ARL. Towards this end, the samples were prepared in a similar way to those used for the optical analysis. Distributions of elements in products of the reaction were also studied. As standards FeS_2 was used for iron and sulphur determination and a metallic silicon for the determination of silicon. Figs. 6 and 7 show the distribution profiles as obtained for the samples sulphidized at 600 and 800° C respectively.

Analysis of the phase composition of the studied layers was carried out by means of X-ray

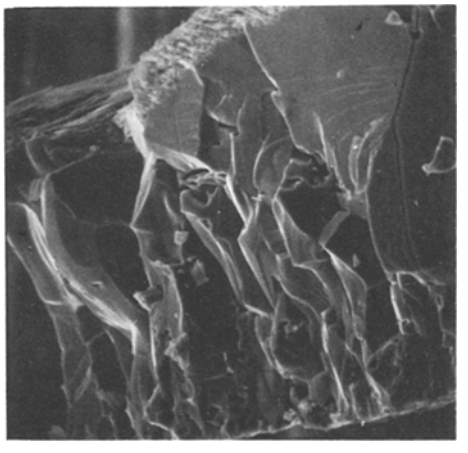

Figure 3 The microstructure obtained from the fracture of the outer scale for $T_s = 800°C$. Note well-formed columnar crystals and a lack of defects.

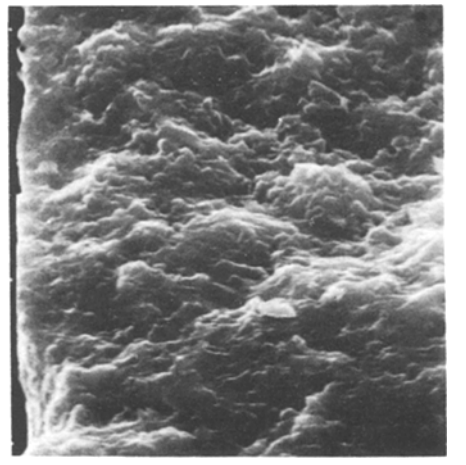

Figure 4 The microstructure obtained from the fracture of the layer occurring on the core for $T_s = 800°C$ (× 600). Irregular thin plates and spheres with numerous pores and discontinuities are characteristic features here.

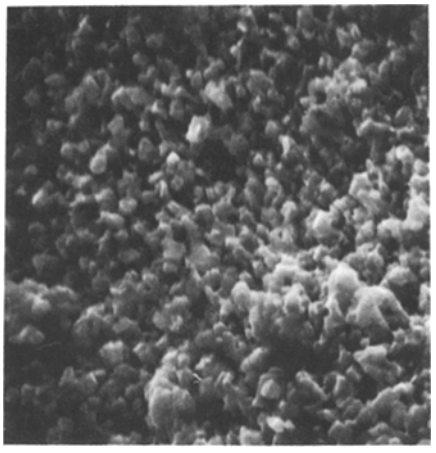

Figure 5 The microstructure obtained from the surface of the core for $T_s = 800°C$ (× 5200). Note small detached sphere-like elements forming this microstructure.

diffraction using a molybdenum tube. The outer layer of the scale had been removed before this analysis was performed. Reflections obtained were interpreted based on ASTM Tables [6]. The X-ray diffraction was carried out on subsequent layers: starting with the inner part of the scale, followed by the layer occurring on the metallic core, and finally with the one of the metallic core itself.

A particular layer was made accessible by grinding the preceding one. This procedure was continued until the diffraction pattern obtained was identical with that characteristic of the initial (unsulphidized) sample.

Fig. 8 shows a phase distribution as deduced from the above study. The kind and relative abundance of phases occurring in the four layers studied can be learnt from it.

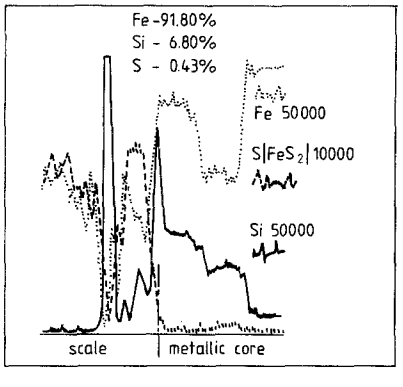

Figure 6 Distribution of elements for the sample sulphurized at $T_s = 600°C$.

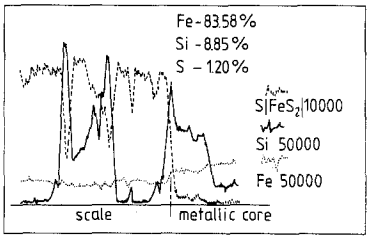

Figure 7 Distribution of elements for the sample sulphurized at $T_s = 800°C$.

For the analysis by means of the Mössbauer spectroscopy, samples in the form of foils were prepared from (a) the surface zone of the core (i.e. the region in contact with the scale), and (b) the inner part of the core, for all the sulphidized samples. In addition, a foil prepared from the unsulphidized sample was investigated too. The foils were prepared by hand-grinding with glasspapers followed by a chemical polishing in a solution of 50 g CrO_3 + 0.45 dm^3 H_3PO_4. During the latter process the outer surface of the sample of the surface zone of the core was covered with a varnish in order to protect it from dissolution.

^{57}Fe Mössbauer spectra were collected at room temperature in a transmission geometry. The 14.4 keV monoenergetic γ rays were supplied by a source of ^{57}Co in a chromium matrix. Its activity was about 20 mCi, and each spectrum was collected with statistics of 7 to 8×10^6 counts per channel. As a calibration standard an iron foil of α-Fe was used. Fig. 9 shows the spectra obtained.

2.2. Chemical composition of the layers of interest

It turns out that in all investigated samples there

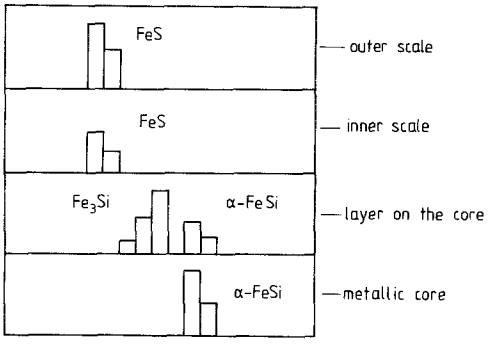

Figure 8 Phase distribution as obtained for the sample sulphurized at $T_s = 800°C$.

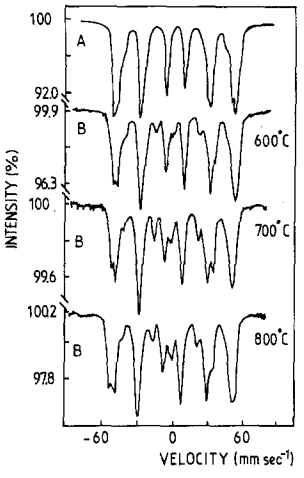

Figure 9 Room temperature Mössbauer spectra of (A) a sample cut out of the central part of the core, and (B) a sample obtained from the surface region of the core for different T_s shown.

is a rather homogeneous distribution of elements within the metallic core. However, in the layer occurring on the core one observes a rather sharp increase in silicon concentration and simultaneously a decrease in the concentration of iron. The sulphur content in this layer increases smoothly when approaching the scale, and its concentration does not exceed 0.5 to 1.5%. In the inner scale there is silicon whose concentration is larger than that within the metallic core, as well as within the layer occurring on its surface. The sulphur content is rather high, excluding regions where silicon is present. Here its concentration is significantly smaller. In the outer scale there is no silicon at all, and the concentration of iron and sulphur corresponds to FeS_2 (see Figs. 6 and 7).

Because of the morphology of the layers, the above results should be treated only qualitatively.

2.3. Morphology of the layers

The morphology of the studied layers was investigated by means of metallographic methods as well as by observing fractures with the scanning electron microscope.

Three layers could be distinguished in all cases: (a) an outer layer of scale, (b) an inner layer of scale, and (c) a layer occurring on the core. The outer scale, being very distinct from the others, is characterized by numerous holes, cracks and pores which must largely be due to the preparation of microsections. The inner scale, being rather thin, looks more compact and homogeneous, and it is less grey than the outer scale. Finally, the third layer, being in consistency similar to the inner scale, is characterized by a metallic lustre. It sticks rather firmly to its predecessor, but it can become relatively easily detached from the metallic core (which in fact occurs in the course of microsection preparation, as shown by Figs. 1 to 3).

The investigation of morphology with the scanning electron microscope was performed on perpendicular fractures of all layers of interest. It turns out that the outer scale is built from well-formed columnar crystals. No holes, cracks or pores have been detected in it which confirms the earlier remark that these defects result from the preparation of the microsection (Fig. 3).

The morphology of the thin inner scale could not be observed with this method. This was most likely due to the fact that it is similar to the morphology of the much thicker layer occurring on the core, the latter being composed of irregular thin plates and spheres and having numerous pores and discontinuities (Fig. 4). The surface of the metallic core, investigated after having removed all previous layers, turns out to be covered with small detached sphere-like elements (Fig. 5).

2.4. Evaluation of the Mössbauer spectra

The spectra were computer-analysed on a superposition principle, i.e. the resultant spectra were regarded as composed of a number of six-line subspectra having characteristic hyperfine (hf) splittings H and isomer shifts I. Each subspectrum was ascribed to an atomic configuration (m, n) of a probe atom having m silicon atoms in the first and n silicon atoms in the second neighbour shell.

It was further assumed that the influence of silicon atoms on the hf parameters is additive, i.e. the following relations hold:

$$H(m, n) = H(0, 0) + m\Delta H_1 + n\Delta H_2 \quad (1)$$

$$I(m, n) = I(0, 0) + m\Delta I_1 + n\Delta I_2 \quad (2)$$

where $H(m, n)$ is the hf field at a ^{57}Fe nucleus in the (m, n) configuration, and $\Delta H_{1,2}$ are the hf field shifts caused by one silicon atom residing in the first (index 1) and in the second (index 2) neighbour shell. The meaning of $I(m, n)$ and $\Delta I_{1,2}$ is similar.

TABLE I Best-fit parameters* as obtained from the Mössbauer spectra for the studied samples

Sample	$H(0, 0)$	ΔH_1	ΔH_2	$I(0, 0)$	ΔI_1	ΔI_2	$\bar{H}_I$	$\bar{H}_{II}$	$\bar{I}_I$	$\bar{I}_{II}$	Q	I
A	337.1	−29.6	−9.2	−0.008	0.04	0.00	–	–	–	–	–	–
B (600° C)	341.0	−32.0	−10.0	0.000	0.04	0.00	315	201	0.07	0.24	0.58	0.26
B (700° C)	336.0	−32.5	−10.7	0.003	0.04	0.01	311	199	0.08	0.24	0.57	0.23
B (800° C)	338.0	−31.0	−11.0	0.000	0.05	0.01	314	202	0.06	0.25	0.59	0.29

*hf fields H are in kOe ($10^6/4\pi$ A m^{-1}), isomer shifts I in mm sec^{-1} and quadrupole splittings Q in mm sec^{-1}. Meanings of the parameters are given in the text.

The resultant spectra were decomposed into six subspectra corresponding to the six most probable atomic configurations for that composition (assuming a random distribution of atoms). However, the relative abundances of these subspectra $P(m, n)$ were parameters to be fitted, to allow thereby for expected changes in the atom distribution due to sulphidation.

Using the above procedure one could satisfactorily fit only the spectrum of the unsulphidized sample (labelled A in Fig. 9). The spectra obtained for the layers of interest of the sulphidized samples exhibit additional lines which could be accounted for by two additional subspectra, possibly related to iron atoms occupying two different sites in the ordered DO_3 structure. It is well known that in this structure there are two nonequivalent iron sites I and II having the following atomic configurations: Fe_I–(4Fe, 4Si; 6Fe), Fe_{II}–(8Fe, 6Si). Their relative intensities are 2 : 1. It has also turned out (see spectra labelled B in Fig. 9) that in the central part of the spectra there is still not a well-resolved additional line which could be well fitted as a doublet.

By means of the least-squares fitting procedure the spectra could now be well fitted. The best-fit parameters are displayed in Table I. Values of the hf parameters $H(0, 0)$, $\Delta H_{1,2}$, $I(0, 0)$ and $\Delta I_{1,2}$ agree well with the corresponding parameters obtained for the unsulphidized sample. Values of the hf parameters obtained for the two additional subspectra are within the error limits identical with those characteristic of DO_3 structure [7, 8]. Finally, parameters characterizing the doublet (Q and I) are in agreement with those characteristic of FeS_2 [9].

Therefore, in order to gain a more quantitative insight into the problem of the development of DO_3 structure under sulphidation we introduce the following order parameters, Ω:

$$\Omega = \frac{\bar{N}_0 - \bar{N}}{\bar{N}_0 - 4.67} \qquad (3)$$

where $\bar{N}_0$ stands for the average number of silicon atoms in the first two neighbour shells as calculated for a random distribution of atoms, and $\bar{N}$ corresponds to the actual distribution, i.e. $\bar{N}$ was calculated from the formula

$$\bar{N} = \sum_{(m,n)} (m + n) P(m, n) \Big/ \sum_{(m,n)} P(m, n) \qquad (4)$$

The Ω parameter is equal to zero for randomly distributed atoms and to unity if the atoms form the DO_3 structure. It has been evaluated for the whole magnetic part of the sample (i.e. the doublet was excluded) as well as for the non-ordered part of the magnetic part of the spectra (i.e. the doublet and the two subspectra characteristic of the DO_3 structure were excluded). In the latter case it has been called Ω' (see Table II), and it measures a departure from a random distribution of atoms within the non-ordered phase in terms of the DO_3 structure. One can readily see from Table II that in fact $\Omega' = 0$.

Finally, a relative abundance of iron atoms in the DO_3 structure, $P(DO_3)$, as well as in the FeS_2 phase, $P(FeS_2)$, have been determined and displayed in Table II. This table contains also values of probabilities $P(0, 0)$ as determined by fitting the spectra. As can be seen, a decrease of $P(0, 0)$ is correlated with an enhanced degree of order Ω.

3. Discussion of results

It follows from the X-ray analysis that sulphidation of an $Fe_{94}Si_6$ alloy at 600 and 800° C

TABLE II Parameters evaluated from Mössbauer spectra. For details see text

Parameter	Sample			
	A	B (600° C)	B (700° C)	B (800° C)
Ω	0.114	0.302	0.408	0.355
Ω'	0.114	0.124	0.113	0.153
$P(DO_3)$	–	0.202	0.332	0.313
$P(FeS_2)$	–	0.024	0.046	0.079
$P(0, 0)$	0.196	0.130	0.110	0.090

results in the development of three layers on the metallic core. The outermost one, called the outer scale, has the phase composition of FeS. The next one, being very thin and called the inner scale, could not be fully identified as far as its phase composition is concerned. When detached, however, from the outer scale it had a smell characteristic of H_2S. In its X-ray pattern there were reflections typical of iron sulphide. Finally, the layer occurring on the core turns out to be a mixture of the ordered structure DO_3 as well as of a nonordered α phase of Fe–Si. No reflections characteristic of FeS or FeS_2 have been detected.

From the analysis of the Mössbauer spectra it follows that the actual composition of the layer on the core depends on the temperature of sulphidation T_s. For $T_s = 700°\,C$, $P(DO_3)$ has its maximum and Ω' its minimum. For $T_s = 800°\,C$ the contribution of the DO_3 structure to this layer decreases at the cost of the FeS_2 phase, whose abundance steadily increases with increasing T_s.

The concentration of silicon in this layer has doubled in comparison with its value inside the core, and the concentration of iron has decreased. There is no simple correlation between the concentration of silicon and T_s.

The concentration of sulphur, being not larger than 2%, increases with T_s and for a given T_s it increases from the core surface in the direction of the inner scale.

In the X-ray pattern of the inner scale there are peaks characteristic of silicon. They may be due to SiO_2 which together with H_2S is a product of the disintegration of SiS_2 in the humid air. This is also evidenced by the smell of H_2S revealed after having removed the outer scale.

In the outer scale, concentrations of iron and sulphur are constant over the whole cross-section of this layer and correspond to iron sulphide. There is no evidence for the presence of silicon in this layer.

4. Interpretation of results

It has been shown that a process leading to the formation of a layer enriched in silicon and containing the DO_3 structure occurs in particular within the surface zone of the metallic core. We believe that it has thermodynamic and kinetic origins. In the following a possible picture of what occurs is given.

A standard enthalpy of FeS formation is smaller than the one needed to form SiS_2. In addition, the activity of silicon in the studied alloy is diminished by its low concentration. According to Barin and Knacke [10, 11], standard enthalpies G for the following reactions at $T = 600$ to $800°\,C$ are as follows:

$$G(\mathrm{Si} + \mathrm{S_2} \rightarrow \mathrm{SiS_2}) = -43.2 \text{ to } -50.3\,\mathrm{kcal\,mol^{-1}} \quad (5)$$

$$G(2\mathrm{Fe} + \mathrm{S_2} \rightarrow 2\mathrm{FeS}) = -70.5 \text{ to } -77.7\,\mathrm{kcal\,mol^{-1}} \quad (6)$$

According to the parabolic law of sulphuration the appropriate constants of a pure iron and α-FeSi at $T_s = 600$ to $800°\,C$ under a pressure of 1 atm are equal to 0.6×10^{-6} to 4.6×10^{-5} for the former [12] and to 0.6×10^{-6} to $2.77 \times 10^{-6}\,g^2\,cm^{-4}\,sec^{-1}$ for the latter [13]. In addition, the sulphidation of pure silicon occurs a few order of magnitudes slower than that of pure iron [14]. From the above data it follows that the rate of sulphidation of the studied alloy is mainly determined by the reaction of iron with sulphur. Consequently, from the very beginning of the sulphidation FeS forms on the surface of the alloy, blocking thereby a further access of sulphur to the metallic surface. As a result of this, SiS_2 cannot be formed and the surface region of the core gets enriched in silicon. Increase of the silicon concentration in Fe–Si alloy leads to ordering of silicon atoms in the matrix. The solid solution of Fe–Si has a bcc structure whose atomic configuration can be described in terms of four sublattices I, II, III and IV having the fcc structure themselves (see Fig. 10). Atoms occupying I and II sites are the nearest neighbours to those residing in III and IV sites, and vice versa. On the other hand, atoms occupying I and III sites are the next-nearest neighbours to the atoms located at II and IV sites.

In order to describe a distribution of atoms within these four sublattices one introduces three parameters x, y and z defined in the following way [2]:

$$\begin{aligned} x &= \tfrac{1}{4}(P_{\mathrm{Fe}}^{\mathrm{I}} + P_{\mathrm{Fe}}^{\mathrm{II}} - P_{\mathrm{Fe}}^{\mathrm{III}} - P_{\mathrm{Fe}}^{\mathrm{IV}}) \\ y &= \tfrac{1}{2}(P_{\mathrm{Fe}}^{\mathrm{III}} - P_{\mathrm{Fe}}^{\mathrm{IV}}) \\ z &= \tfrac{1}{2}(P_{\mathrm{Fe}}^{\mathrm{I}} - P_{\mathrm{Fe}}^{\mathrm{II}}) \end{aligned} \quad (7)$$

where P_{Fe}^{i} is the probability of having an iron atom in the ith sublattice (i = I, II, III, IV).

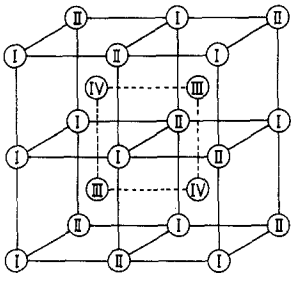

Figure 10 Spatial arrangement of the sublattice sites I, II, III and IV.

If $x = y = z = 0$ the lattice is called A2. If $x \neq 0$ and $y = z = 0$, iron atoms preferentially occupy I and II ($x > 0$) or III and IV ($x < 0$) and the structure is called B2. Consequently, silicon atoms can occupy Sites III and IV or I and II, respectively. As a result of this selective site occupation the number of Fe–Si near-neighbour pairs increases in comparison with the situation in A2.

If $y \neq 0$ or $z \neq 0$ the existing structure is called DO_3 and its characteristic feature is that the number of the next-nearest Fe–Si pairs is larger than that for B2. (Sites III and IV are occupied by Fe_I atoms, Sites II by Fe_{II} atoms, and Sites I by silicon atoms.)

As shown in the present study, the sulphidation results in a formation of the above superstructure in the surface zone of the core.

Because of a high affinity between silicon and iron which is due to interaction between 3s–3p electrons of silicon with 3d ones of iron, there will be a tendency for silicon atoms to "bind" neighbouring iron atoms. In fact, a strong interaction between iron and silicon atoms has been reported [15, 16]. Consequently, only those iron atoms which do not participate in the formation of the superstructures will react with sulphur atoms forming FeS and causing thereby a relative increase of silicon content. Its maximum occurs at the interface metallic core/layer on the core. At this interface the concentration of sulphur is sufficient to react with iron atoms not participating in the formation of the superstructures. A flux of vacancies resulting from a transfer of iron atoms from the core into the scale and flowing in the opposite direction may also help to form the superstructures; they enhance the mobility of the atoms, making thereby a formation of new atomic configurations easier.

The actual abundance of DO_3, $P(DO_3)$, is determined by at least two competing phenomena: its formation and its decay. From the corresponding $P(DO_3)$ values displayed in Table II it follows that (a) for $T_s = 600$ to 700° C the rate of formation R_f is larger than the decay rate R_d, and (b) for $T_s = 700$ to 800° C $R_f < R_d$.

The decay of the DO_3 structure occurring at the interface inner scale/layer on the core is due to the activity of sulphur in this region as well as to a high mobility of iron atoms in FeS, and of silicon atoms in the SiS_2. Iron atoms in FeS diffuse faster ($D_{FeS} = 3.7 \times 10^{-7} cm^{-1}$ [17]) than those in the α-FeSi phase ($D_{FeSi} = 3.2 \times 10^{-11} cm^{-1}$ [18]), and probably also those in DO_3. As a result of this diffusion, iron atoms quickly reach the outer scale where after having reacted with sulphur they increase the thickness of the outer scale, or react with sulphur originating from a dissociation of the outer scale, and finally form FeS which remains in the inner scale.

The activity of sulphur at the interface metallic core/scale is, in the equilibrium condition, equal to the decay pressure of the iron sulphide. When forming superstructures the activity of sulphur is even larger, because DO_3 decays into FeS and SiS_2 (SiS_2 can be more easily formed from DO_3 than from α-FeSi because the chemical potential of silicon in DO_3 is larger than that in α-FeSi). This is due to the existence of dissociation fissures along which sulphur can quickly diffuse into the zone of metal consumption [19].

5. Conclusions

Based on the results obtained in the present investigation and presented in previous sections, the following conclusions can be drawn:

1. Sulphidation of an $Fe_{94}Si_6$ alloy leads to enrichment of the surface region of the metallic core in silicon, and subsequently to a formation of DO_3 structure in that region.

2. The main reason for this enrichment is a selective sulphidation of iron atoms taking place on the core surface.

3. Vacancies being created on the surface of the core catalyse ordering of the alloy in the DO_3 structure.

4. DO_3 structure formed at the interface inner scale/metallic core decays into FeS and SiS_2.

Acknowledgements

We are grateful to Professor T. Werber for his stimulating interest in this work and to Dr Ing. S. Bzowski for illuminating discussions on the problem of superstructures.

References

1. M. SCHMAHL, H. BAUMAN and H. SCHENCK, *Z. Elektrochem.* **63** (1959) 855.
2. G. INDEN and W. PITSCH, *Z. Metallkde.* **62** (1971) 627.
3. T. WERBER and Z. ŻUREK, to be published.
4. S. M. DUBIEL, T. WERBER and Z. ŻUREK, "Proceedings of the 8th International Congress on Metallic Corrosion", Mainz, 1981, edited by Dechema (Frankfurt/Main, 1981) p. 815.
5. S. MROWEC and T. WERBER, *Chem. Anal.* **7** (1965) 605 (in Polish).
6. "ASTM Data", edited by Joint Committee on Powder Diffraction Standards (American Society for Testing and Materials, Philadelphia, 1979).
7. M. B. STEARNS, *Phys. Rev.* **168** (1968) 588.
8. MON-CHING LIN, R. G. BARNES and D. R. TORGESEN, *Phys. Rev. B* **24** (1981) 3712.
9. A. A. TEMPERLEY and H. W. LEFEVRE, *J. Phys. Chem. Solids* **27** (1966) 85.
10. J. BARIN and O. KNACKE, "Thermochemical properties of inorganic substances" (Springer Verlag, New York, 1973) p. 297.
11. *Idem, ibid.*, p. 692.
12. M. DANIELEWSKI, *Bull. Acad. Pol. Sci.* **5** (1979) 425.
13. Z. ŻUREK, unpublished results (1984).
14. *Idem*, to be published.
15. M. B. STEARNS, *Phys. Rev.* **147** (1966) 439.
16. F. KÖRBER and W. OELSEN, *Mitt. Kaiser Wilhelm Inst. für Eisenforsch.* **18** (1936) 109.
17. E. FRYT, W. W. SMALTZER and J. S. KIRKAIDY, *J. Electrochem. Soc.* **126** (1979) 673.
18. C. J. SMITHELLS, "Metals Reference Book" (Butterworths, London, 1976) p. 897.
19. T. WERBER, *Zesz. Nauk. AGH (Ceramika)* **23** (1972) 39 (in Polish).

Received 11 September
and accepted 18 December 1984